



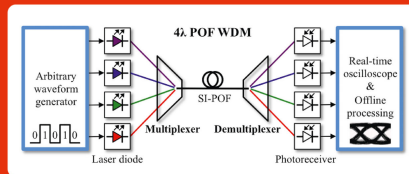
Mladen Jončić (Autor)

Wavelength Division Multiplexing for Short-Range Communication Over 1 mm Step-Index Polymer Optical Fiber

Lehrstuhl für Kommunikationstechnik NO. 14, 2016
Hochschule Harz (FH)

U.H.P. Fischer-Hirchert (Hrsg.)

Wavelength Division Multiplexing for Short-Range Communication Over 1 mm Step-Index Polymer Optical Fiber



Mladen Jončić



Cuvillier Verlag Göttingen
Internationaler wissenschaftlicher Fachverlag

<https://cuvillier.de/de/shop/publications/7191>

Copyright:

Cuvillier Verlag, Inhaberin Annette Jentzsch-Cuvillier, Nonnenstieg 8, 37075 Göttingen, Germany

Telefon: +49 (0)551 54724-0, E-Mail: info@cuvillier.de, Website: <https://cuvillier.de>



1 Introduction

Having its origin in the 1960's as well as the silica glass fiber, the polymer optical fiber (POF) stayed long in the shadow of the huge development and success of glass fiber communications. However, the advances in POF technology and the growing need for high-speed short-range communication networks make POF nowadays gain more and more in importance. The key advantage of POF is a large core diameter. It makes POF tolerant to the fiber facet damages and relaxes the alignment tolerances, thus also reducing the installation costs. Furthermore, POF is pliable, durable, and inexpensive, offers small weight and short bend radius, allows easy installation, simple termination and quick troubleshooting, and also provides the immunity to electromagnetic interference. Due to its diverse advantages, in short-range applications POF established itself as a reasonable alternative to the traditional data communication media such as glass fibers, copper cables and wireless systems (see Table 1.1).

Table 1.1: Comparison of different transmission media. Characteristics between very bad (--) and particularly good (++) [Fischer11].

Transmission medium	Data rate	Distance	Safety	Cost	Handling	Installation	Total
Twisted pair cable	+	0	0	++	-	0	2+
Coaxial cable	0	0	0	+	0	0	1+
Glass fiber	++	++	++	--	--	-	1+
Polymer fiber	0	-	++	+	+	+	4+
Wireless	--	-	--	++	++	++	1+
Powerline	-	-	--	+	+	++	0

Today, POF is produced with different core materials, core diameters and index profiles. A comprehensive overview on various POFs is given in [Ziemann08]. Two major POF types are made of polymethyl methacrylate (PMMA) and perfluorinated (PF) materials. The parameters of the common PMMA and PF POFs are specified in the IEC Standard 60793-2-40, which defines eight different POF classes [IEC09].

The PMMA POF is produced with both step-index (SI) and graded-index (GI) profile, whereas the PF POF offers only GI profile. The GI profile of the core ensures high modal bandwidth exceeding $1.5 \text{ GHz} \times 100 \text{ m}$ for the PMMA POF and $300 \text{ MHz} \times 1 \text{ km}$ for the PF POF. However, the implementation of the PMMA GI-POF is confined to 500-680 nm wavelength range due to the high optical attenuation at other wavelengths ($> 400 \text{ dB/km}$). The



PF GI-POF is best suited for use in the infrared region, e.g. in the first (850 nm) and the second (1300 nm) optical window, where of-the-shelf components developed for multimode glass fibers are available. In contrast, the PMMA SI-POF suffers from intermodal dispersion limiting the bandwidth-length product to around $50 \text{ MHz} \times 100 \text{ m}$ (see subchapter 2.1), but also provides several attenuation windows in the visible spectrum (400-700 nm). Due to its advantages over the other POF types such as technological maturity, ease and cost of production and high numerical aperture (NA), the standard 1 mm PMMA SI-POF (POF class A4a.2 according to IEC 60793-2-40) is the best known and by far the most widely employed type of POF. This is also the fiber the thesis concentrates on. Throughout the work the terms SI-POF and POF will be equally used to address this fiber type.

Three major application sectors of SI-POF data communication technology are industrial automation, automotive industry and in-house/office networks. Over more than 25 years SI-POF has been employed in industrial automation applications. The bus systems such as Profibus (1.5 Mb/s, 60 m) and INTERBUS (2 Mb/s, 70 m), and industrial Fast Ethernet (100 Mb/s, 50 m) are the typical application scenarios.

In vehicles SI-POF displaces copper in the network structure of a passenger cabin for multimedia data services. The infotainment communication system known as Media Oriented System Transport (MOST) connects different multimedia components in the SI-POF-based ring topology [Grzempa08], as illustrated in Fig. 1.1. First introduced in the BMW 7 Series 2001, the MOST technology is nowadays used by almost all major car manufacturers in the world. In 2011 there were more than 50 different car types on the market employing SI-POF (BMW, Mercedes-Benz, Ford, Hyundai, etc.) [Bunge12]. The current (third) version of the MOST system (MOST150) supports the data transfer at 150 Mb/s over link lengths of about

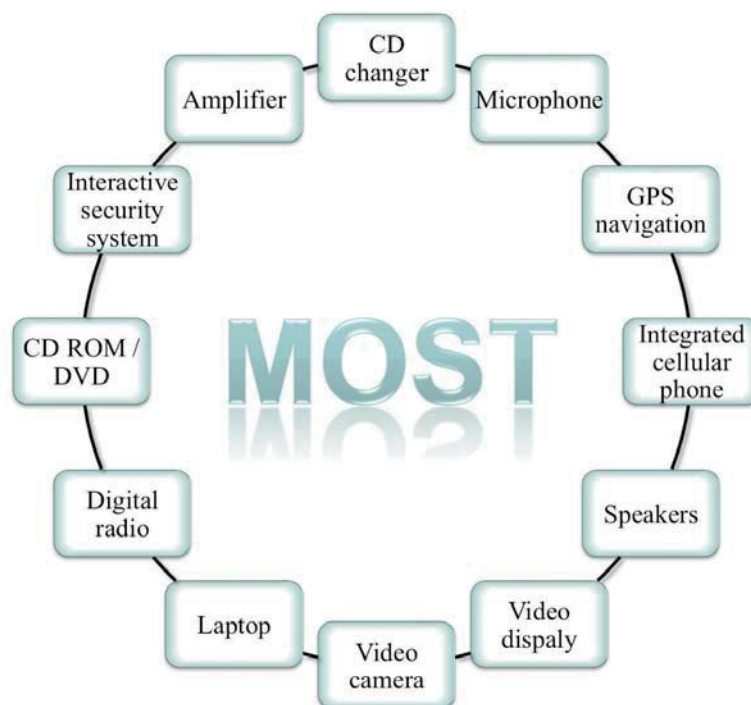


Fig. 1.1: SI-POF-based ring topology of a MOST system in a car.

10 m. Not only multimedia, but also security-critical and safety applications benefit from SI-POF (e.g. Byteflight bus system, 10 Mb/s).

Another sector where SI-POF displaces traditional communication media are short-range networks in houses and offices. As an in-house extension of a broadband access network (e.g. VDSL, HFC, FTTB), the typical application of POF technology is the delivery of triple-play services (combination of broadcasting, telecommunication and internet) to the end user, as illustrated in Fig. 1.2. The Fast Ethernet transceivers (100 Mb/s) and since 2013 also the Gigabit Ethernet transceivers (1 Gb/s) are available on the market enabling the transmission of broadband services over 50 m SI-POF. The Gigabit solutions from KD-POF employing the multilevel signaling and from Teleconnect based on the multicarrier modulation are accompanied by the technical standards ETSI TS 105 175-1-2 [ETSI15] and ITU-T G.9960, Annex F [ITU11], respectively.

The commercial communication systems with SI-POF use a single channel for data transmission. However, the transmission performances of SI-POF are impaired by strong inter-modal dispersion and high optical attenuation. Stimulated by the growing bandwidth demands (e.g. 10 Gb/s to 40 Gb/s to 100 Gb/s Ethernet speed), various concepts to overcome the low-pass characteristic of SI-POF have been successfully demonstrated over the last few years. The simplest solutions utilized passive equalization implemented as an analog high-pass filter that increased the electrical -3 dB bandwidth of a channel [Vinogradov08]. A similar approach but with an adaptive analogue equalizer was presented in [Sundermeyer09]. Other solutions concentrated on the development and optimization of the fast transceiver components including a red vertical-cavity surface-emitting laser [Johnson12], a large-area photodetector [Loquai14], or even a fully integrated photoreceiver with adjustable equalizer [Atef12]. A major focus was also placed on the digital signal processing techniques, which were mostly implemented offline due to the lack of commercial components. Both the non-

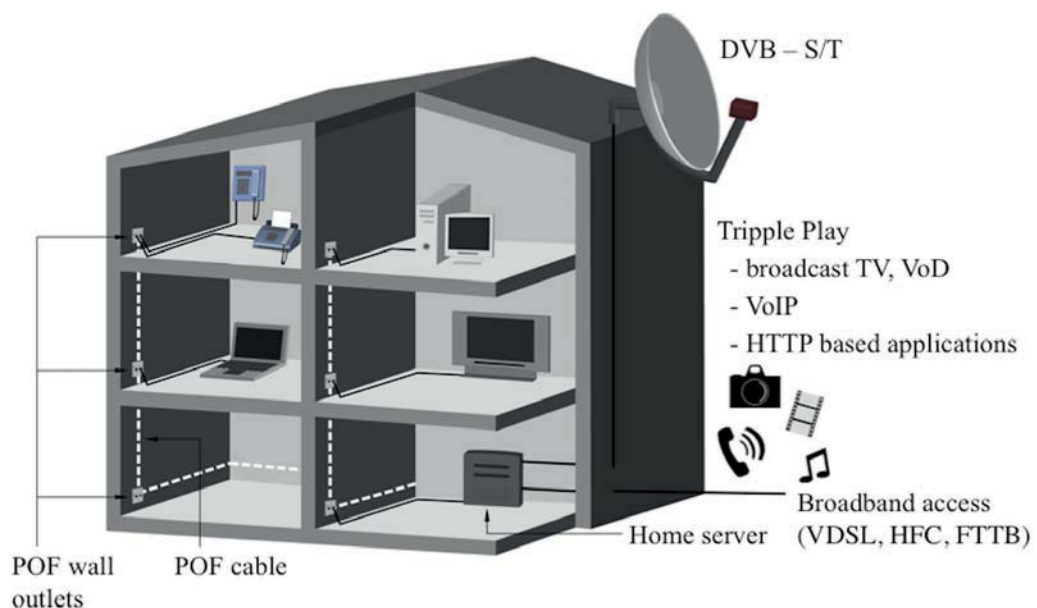


Fig. 1.2: In-house communication scenario with Ethernet over POF.



return-to-zero (NRZ) and the spectrally efficient multilevel signaling were combined with the digital receiver equalization to increase the data rates over SI-POF [Loquai13], [Breyer10]. The sophisticated spectrally efficient multicarrier modulation formats were also successfully implemented to combat the highly dispersive SI-POF channel [Lee09a], [Vinogradov11]. A record capacity of approx. 6.3 Gb/s was achieved over 50 m SI-POF at the bit error rate (BER) of 10^{-3} employing the offline-processed discrete multitone (DMT) modulation and a commercial 650 nm laser diode [Vinogradov11]. In the same publication, a record capacity of approx. 4.2 Gb/s was demonstrated over 100 m SI-POF at the BER= 10^{-3} , allowing for error-free transmission after implementing forward-error correction (FEC). An early prototype of OSRAM 515 nm laser diode was thereby employed to transmit NRZ signal, which was equalized at the receiver using the offline implementation of a decision-feedback equalizer (DFE).

Complying with any of the hitherto developments, utilization of several optical carriers for parallel transmission of data channels over a single fiber represents another alternative to increase the transmission capacity of SI-POF. The technique is well known as wavelength division multiplexing (WDM). In glass fiber communications WDM has been firmly established for more than two decades and represents the key technology in modern high-capacity optical networks with the distances ranging from several thousand down to ~ 10 km [Mukherjee06], [Kartalopoulos02], [Thiele07]. The principle of WDM is shown in Fig. 1.3. Since different wavelengths λ_1 – λ_N do not interfere with each other in a linear medium, they can be used to simultaneously carry the data signals over a single fiber. Thereby, the capacity of a fiber i.e. of an optical communication system increases almost proportionally with the number of wavelength channels.

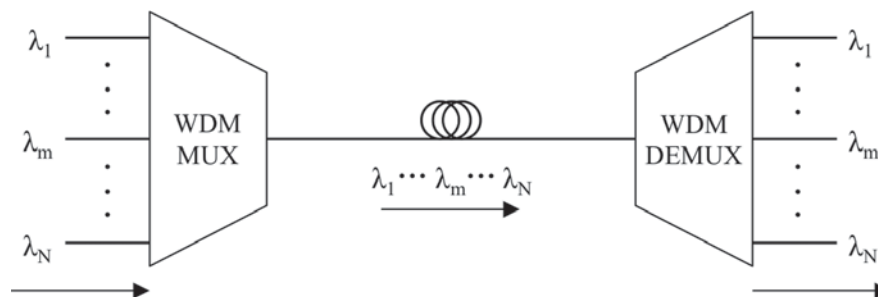


Fig. 1.3: Principle of WDM: MUX – multiplexer; DEMUX – demultiplexer.

Two components are essential for WDM, a wavelength multiplexer and demultiplexer. The multiplexer combines the signals at different wavelengths, coming from different transmitters, onto a single fiber. On the opposite side of the optical link the demultiplexer performs an inverse function, separating the wavelength channels to be detected by separate receivers. Because of e.g. interchannel crosstalk, the demultiplexer is more often considered in fiber optics. Therefore, this thesis concentrates on the demultiplexing function without loss of generality for the multiplexing operation.



The existing WDM components developed for single-mode glass fibers in the infrared region, such as Mach-Zehnder interferometers, arrayed waveguide gratings or fiber Bragg gratings, cannot be reused for a highly multimode SI-POF. On the other hand, the operating principles of demultiplexers based on thin-film interference filters and on a diffraction grating can be applied for POF. In spite of some other demultiplexing solutions (e.g. employing dispersion prisms), these two demultiplexing techniques have been recognized as the most promising for SI-POF. However, because of the difference in the operating wavelength range, fiber diameter, NA, etc. compared to the glass fibers, such demultiplexers must be newly designed for SI-POF communication. The subchapters 2.2.1 and 2.2.2 give an overview of the state of the art thin-film interference filter- and diffraction grating-based SI-POF demultiplexers respectively. The first aim of this thesis is to further investigate experimentally these two demultiplexing techniques for SI-POF.

The most frequently mentioned motivation for POF WDM is to increase the transmission capacity of SI-POF link compared to the single-wavelength systems. So far, only a few attempts have been made to investigate that possibility, primarily because of the lack of functional low-loss multiplexing and demultiplexing components. In the early attempts, the light emitting diode (LED)-based POF systems exploiting WDM technology could not provide sufficient capacity [Junger02], [Appelt02], [Bartkiv03]. Only recently, supported by the advance in the visible laser diode technology, the record-breaking POF WDM transmission experiments, including the work of the author, were performed [Kruglov12a], [Kruglov14], [Jončić14b], [Jončić14c]. Accordingly, the second aim of this thesis is to demonstrate experimentally high-speed POF WDM data transmission offering capacity increase compared to the single-channel systems. The third aim of the thesis is to investigate possible channel allocation for today's and future POF WDM systems.

The rest of the thesis is organized in the following manner. Chapter 2 gives the fundamentals of WDM for short-range communication over SI-POF that are used throughout the thesis. The next two chapters consider two different demultiplexing techniques. Chapter 3 focuses on the experimental realization of SI-POF demultiplexer employing thin-film interference filters. In a step-by-step approach, intermediate solutions with two and three channels are first established. In addition, two different configurations of a target demultiplexer setup with four channels are realized and mutually compared. Chapter 4 addresses a theoretical and experimental analysis of the previously produced SI-POF demultiplexer based on a concave diffraction grating. Two methods for characterization of transmission properties of the demultiplexer are proposed and investigated. The measurement results are interpreted in relation to the theoretical calculations and optical simulations, and are used to qualify the manufacturing process. Chapter 5 presents four-channel POF WDM transmission experiments using the demultiplexer introduced in chapter 3 to separate the wavelength channels. Several optimization steps with intermediate results are shown before a target experimental setup and data transmission results are presented, demonstrating the feasibility and potential of a high-speed POF WDM concept. Chapter 6 investigates spectral grids for the visible spectrum WDM applications over SI-POF. Criteria for evaluating the applicability of a grid for the



intended application are defined prior to establishing and analyzing different WDM channel allocations. Finally, chapter 7 summarizes the contributions of this work and outlines the possibilities for the follow-up research.

2 Fundamentals of WDM for short-range communication over POF

This chapter introduces the fundamentals of POF WDM relevant for this thesis. First, the transmission characteristics of SI-POF are considered in terms of optical attenuation and electrical bandwidth. Next, the demultiplexing techniques based on thin-film interference filters and a concave diffraction grating are described. Two data transmission techniques for increasing the channel capacity are then discussed. Finally, an overview of the existing WDM-related standards for glass fiber communication is given.

2.1 Transmission properties of 1 mm PMMA SI-POF

The 1 mm PMMA SI-POF is the best known and by far the most widely employed type of POF. It is made of 980 μm diameter PMMA core surrounded by a thin cladding (10 μm) made of fluorinated polymer. The typical spectral attenuation of SI-POF is shown in Fig. 2.1. The fiber supports operation in the visible spectrum from 400 nm to 700 nm. The lower wavelength bound is determined by the degradation of the PMMA compound with prolonged exposure to the ultraviolet (UV) wavelengths [Lekishvili02]. The attenuation value of around 400-450 dB/km, that still allows operation over shorter link lengths (< 20 m), sets the upper wavelength bound.

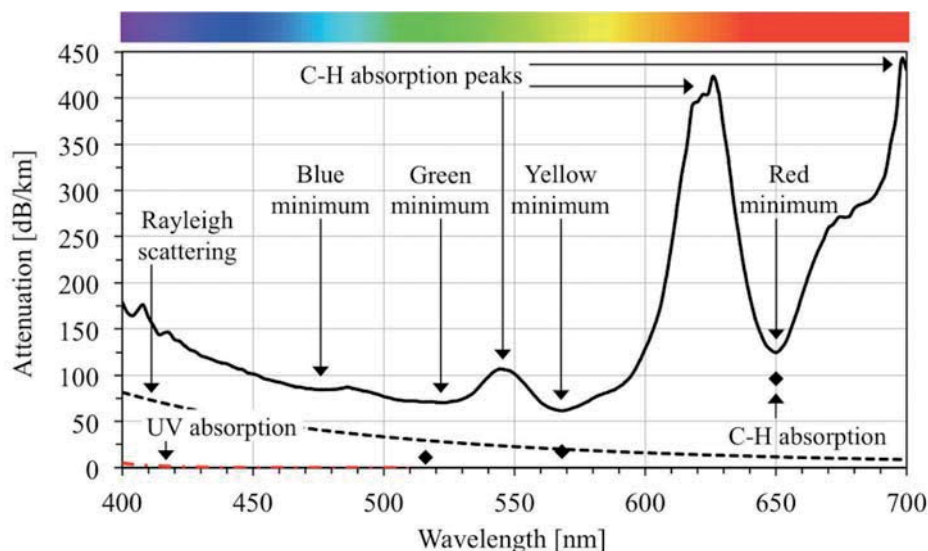


Fig. 2.1: Typical spectral attenuation of 1 mm PMMA SI-POF [Bunge11] with contributions of intrinsic loss mechanisms and with attenuation minima and maxima.



Two intrinsic loss mechanisms contribute to the raise of attenuation at shorter and particularly UV wavelengths. The electronic transitions due to the absorption of light in the polymer compound cause absorption peaks in the UV region. However, their absorption tails extend through the visible spectrum affecting the POF attenuation [Zubia01]. The dependence of the attenuation coefficient of electronic transitions α_e [dB/km] on the wavelength for PMMA is given by [Koike14]:

$$\alpha_e = 1.58 \cdot 10^{-12} \exp\left(\frac{1.15 \cdot 10^4}{\lambda}\right). \quad (2.1)$$

The second loss mechanism is the Rayleigh scattering. It is caused by the structural irregularities in the polymer compound that are much smaller than the wavelength of light (order of one tenth of wavelength or less). The effect of scattering becomes more pronounced as the wavelength decreases since the scattering attenuation coefficient α_s [dB/km] is inversely proportional to the fourth power of the wavelength [Kaino97]:

$$\alpha_s = 13 \cdot \left(\frac{633}{\lambda}\right)^4. \quad (2.2)$$

In the infrared region the attenuation significantly increases due to the intrinsic absorption losses caused by vibrations of the molecular C-H bonds (total of eight per MMA monomer). The higher overtones of the C-H bond vibrations also extend in the visible spectrum. The 7th overtone at 549 nm, and particularly the 6th and the 5th overtone at 627 nm and 736 nm respectively, cause pronounced absorption peaks and wide absorption bands, predominantly determining the level of attenuation in the red spectral range [Emslie88], [Groh88].

The contributions of the intrinsic loss mechanisms to the overall attenuation of SI-POF are also shown in Fig. 2.1. The attenuation contributions due to the vibrations of C-H bonds at 516 nm, 568 nm and 650 nm are taken from [Kaino97]. The sum of individual intrinsic loss mechanisms corresponds to the theoretical loss limit and equals approx. 40 dB/km, 37 dB/km and 107 dB/km at the respective wavelengths. In practice is this limit never achieved due to the extrinsic loss processes (absorption due to impurities in the fiber core, scattering loss due to waveguide structural imperfections, etc.) [Zubia01].

The wavelength regions where the fiber exhibits low attenuation are called attenuation windows. The SI-POF has four attenuation windows. Those are blue, green, yellow and red windows, with the absolute attenuation minimum of approx. 62 dB/km at around 568 nm (yellow window). The parameters of the attenuation windows are listed in Table 2.1.

Table 2.1: Attenuation windows of SI-POF (based on the attenuation curve from Fig. 2.1).

Attenuation window	blue	green	yellow	red
Attenuation minimum [dB/km]	85	70	62	125
Wavelength of the attenuation minimum [nm]	476	522	568	650
Approximate 3 dB width of the window [nm]	19	24	8	4



The mean refractive index of SI-POF core material in the visible spectrum is $n_{core}=1.492$, whereas the refractive index of cladding is $n_{clad}=1.412$. Due to the big difference in refractive indices of core and cladding, the numerical aperture (NA)

$$NA = \sqrt{n_{core}^2 - n_{clad}^2} \quad (2.3)$$

has the value of 0.482 (usually rounded to 0.5). The corresponding maximum acceptance angle of the fiber is 30° . The large core radius $a_{core}=490 \mu\text{m}$ combined with the high NA results in the normalized frequency V

$$V = 2\pi \frac{a_{core}}{\lambda} \cdot NA \quad (2.4)$$

of 2698 at 550 nm, which is far above the limit $V=2.405$ below which a fiber is single-moded. The number of modes N_{mod} propagating through SI-POF can be approximated as

$$N_{mod} \approx V^2/2, \quad (2.5)$$

corresponding to 3.64 million modes at 550 nm. Due to the significant path difference between lower and higher order modes, propagating respectively at smaller and larger angles relative to the optical axis, the strong intermodal dispersion is inherent to SI-POF. In the time domain it is manifested as pulse broadening, thus introducing the inter-symbol interference (ISI). In the frequency domain the intermodal dispersion results in a low pass frequency response, constraining the bandwidth-length product of SI-POF to around $50 \text{ MHz} \times 100 \text{ m}$ [Ziemann08].

2.2 Demultiplexing for 1 mm PMMA SI-POF

The WDM is one possibility to increase the data carrying capacity of SI-POF. The key component for WDM is a wavelength demultiplexer. Different approaches for realization of the demultiplexer for SI-POF have been investigated, including demultiplexing based on a dispersion prism, thin-film interference filters, and a diffraction grating (plane or concave).

The prism-based two-channel demultiplexer operating with LEDs at 530 nm and 650 nm was reported in [Zhang05]. The insertion loss (IL) and the crosstalk were around 17-20 dB and -20 dB respectively. Another solution employing the dispersion prism was shown in [Lutz05]. The three-channel demultiplexer operated with LEDs at 470 nm, 520 nm and 650 nm. It provided the IL of 12-20 dB, whereas the crosstalk took values between -4.6 dB and -34.8 dB. High IL and considerable crosstalk were caused by unoptimized optical components, broad LED spectra and high alignment sensitivity of both setups.

The two other demultiplexing techniques have been recognized as the most promising for SI-POF and have been the most investigated so far. This thesis focuses on the demultiplexers employing interference filters and a diffraction grating, in particular the concave one.



2.2.1 Demultiplexing employing thin-film interference filters

The technology based on thin-film interference filters is mature and one of the most commonly applied technologies for realization of WDM demultiplexers in single-mode glass fiber communication. The demultiplexers for *Coarse* WDM applications cascade the interference filters to provide up to 16 flat-top channels between 1271 and 1611 nm, with 20 nm minimum channel spacing [Thiele07]. The typical parameters of commercial 4-, 8-, and 16-channel demultiplexers with IL less than 1.6 dB, 2.7 dB and 3.7 dB respectively, can be found in [Lightel15]. The thin-film filter-based demultiplexers for *Dense* WDM applications are commercially available with up to 40 channels in 1550 nm region and less than 8 dB IL. Instead of simply cascading the filters, those devices usually employ a modular configuration described in [Dutta03]. The same reference provides a typical transfer function of the 40-channel demultiplexer with 3-6 dB IL and 100 GHz (0.8 nm) channel spacing.

In the visible spectrum, and thus within the application range of SI-POF, a vast variety of thin-film interference filters is available from various manufacturers. Even though not particularly intended for POF applications, the visible interference filters represent an attractive solution for POF demultiplexers, where wavelength selectivity, low IL and high isolation are required.

An interference filter, typically designed for 0° angle of incidence (AOI), utilizes the principle of constructive and destructive interference to selectively transmit certain wavelengths and reject (diminish in intensity and reflect) the others [Macleod10]. Its basic structure comprises multiple thin dielectric layers with alternating high and low refractive indices, which are successively deposited on a single glass substrate. The desired spectral response is obtained by a careful selection of the number of dielectric layers, their thickness and refractive indices. The filter is typically characterized with high passband transmittance ($> 90\%$), steep transition slopes (> 3 dB/nm) and deep blocking (> 30 dB) in rejection bands (see Fig. 2.3).

A dichroic mirror is a special type of interference filter intended for the spatial separation or combination of light at different wavelengths. It is designed to operate at 45° AOI, such that a certain spectral range is transmitted, whereas the rejected wavelength range is reflected at 90° angle with respect to the incident optical axis. A commercial visible spectrum dichroic mirror has a transition slope between the transmission and reflection band of typically 30-40 nm (see Fig. 2.3 and Table 3.1). This is significantly less steep compared to the standard interference filters designed for the normal incidence. Unlike an interference filter, e.g. a longpass mirror must be not only highly transmissive above the cutoff wavelength, but also highly reflective below it. Therefore, producing steeper slopes would require increased complexity of the coating, and accordingly, a significant rise in production costs.

The interference filters show significant angular dependence of their transmission characteristic [Herbert06]. To be applicable for SI-POF, the highly divergent beam from the fiber must be transformed into a bundle of parallel rays prior to the incidence. The principle of separation of two collimated wavelength channels using a dichroic mirror is shown in Fig. 2.2. To increase the channel isolation, an additional bandpass filtering in each of the